Data Analysis of 2D–SAXS Patterns with Fibre Symmetry from Some Elastomers

N.Stribeck

Universität Hamburg, Institut für Technische und Makromolekulare Chemie, Bundesstr. 45, D–20146 Hamburg, Germany

Using a special programming tool for scientific use (PV-WAVE), a program is being developed in order to analyse quantitatively 2D SAXS patterns with fibre symmetry. As the first detectors for synchrotron radiation have become available which allow the recording of high resolution patterns with a good S/N ratio in a short time, there is an urgent need for such evaluation tools. Using data recorded during the straining of two thermoplastic elastomers, the program and the underlying concepts are presented.

1. Experimental

The soft/hard domain structures of two polyetheresters (Sample PBT/PEG from S. Fakirov's laboratory and the commercial product A2000/20 manufactured by DSM) are studied at HASYLAB, beamline A2 using small-angle X-ray scattering (SAXS). The samples are strained in the synchrotron beam and 2D scattering patterns are recorded on image plates. Additional data are recorded in order to eliminate the empty scattering background and to calibrate the intensity with respect to constant primary intensity and constant irradiated volume. The distance between sample and detector is about 1.8m. The usable area of the pattern is limited by the vacuum tube (10cm diameter) and the primary beam stop. The plates are scanned using a Molecular Dynamics model 400 scanner and the program ImageQuant (V3.3). It only requires a square of 12x12cm to be read for a 1.6MB data file in 16bit TIFF format ("gel format") to be generated.

2. Choice of the programming tool

Experience has shown that program code which is relevant for the technique of data evaluation comprises only a rather small part of the whole program, if the coding is done in one of the common languages like Pascal or C. Moreover, in some popular operating systems with a graphical user interface (GUI) one finds serious flaws in the routines for heap memory management, which cause extra programming work. I thus decided to use UNIX based versions of the programming tool PV-WAVE, distributed by Visual Numerics Corp.

Presently my program is simply a collection of procedures and functions, which are called from the interpreter prompt. The advantages of PV-WAVE are, in particular, short development cycles, the extensive library and the close relation to the programming language IDL, another well-known programming tool for the scientist. In order to be able to write effective programs for PV-WAVE, one has to understand the paradigms of a programming language designed for the evaluation of vectors and matrices.

3. Data structure and file format

Basic decisions, such as how to define data structure and how to store data in a file, have far-reaching implications. Bad data structure design results in programs which force the user to process every single dataset sequentially. Good data structure design may allow the user to find his own path through the program without driving it into an inconsistent state. Thus pixel size and other parameters are stored inside each image structure, which may be extended.

Each of the evaluated patterns has to be archived. Each pattern is stored in a file of its own and the complete data structure (pixel values and pattern parameters) is mapped without any conversion into the file. Thus even large images can be read and stored fast. Representations of floating point numbers and even of integers (big-endian vs. little-endian) vary from platform to platform (e.g. UNIX on an Intel-based machine and UNIX on a Silicon Graphics workstation). In order to read files across platforms using PV-WAVE, the interpreter offers a special binary format named "exchange data format". This format enables any local PV-WAVE interpreter to convert foreign binary formats transparently into the local binary representations.

In fact, the achieved portability is not really far–reaching, since the algorithms rely on a particular data structure. Thus a new island solution is created. A major reason for this presentation was my interest in a discussion which may lead to a redesign according to a common proposal of an interchange data format for 2D scattering patterns.

Generation and definition of my image data structure can be extracted from the following:

```
; img=sf_structure( $
; 'Sample', '19961001', $
; 500, 450 )
; Generates a
; sf_structure with
; img.Width = 500
; img.Height = 450
; img.map (all zero
; floating point matrix)
; img.BoxLen = (0, 0)
; (floating point vector)
; img.Center = (0, 0)
; (integer vector)
; img.Title = 'Sample'
; img.Date = '19961001'
;
FUNCTION sf_structure, $
 name, stamp, x, y
; Generate structure and
; fill in parameter values
 RETURN, $
  { , Width:x, $
    Height:y, $
    map:FLTARR(x,y), $
    BoxLen:FLTARR(2), $
    Center:INTARR(2),$
    Title:name, $
    Date:stamp }
END ; Func sf_structure
```

4. Raw data features

The scanned scattering pattern is given in a gel format file (eww480r.gel) and must be mapped onto an image structure (e.g. r480) in computer memory (r480 = sf_gelread('sbb20_4a.gel')). Then library functions of PV-WAVE can be used to display a topographical plot of the pattern on the screen. The features of the pattern determine the first steps of data evaluation (see figure 1).

4.1 Shade of vacuum tube and background fog

A relatively large area outside a circle is shaded by the vacuum tube. Here we loose information on the scattering, but gain information on the height of the background fog level. Thus background fog can easily be subtracted from every pattern.

The sharp shadow boundary can be used to align sample scattering and empty scattering before correction. This is necessary, since the positions of

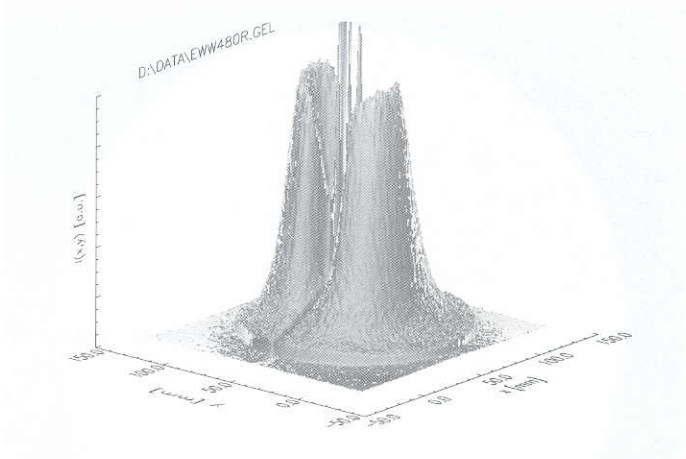

Figure 1: Raw SAXS data of a PBT/PEG, 1min after recovering from an elongation ε=1.48. Image plate exposure: 2min.

the patterns vary from gel file to gel file. By extrapolating a surface into the blind outer region it may be possible to extend information on the shape of the scattering.

4.2 Pattern tilt

In general, the main axis of the straining stage is not parallel to the y-direction of the scanned image. Thus provisions must be made which allow correction for a tilt angle from symmetry considerations.

4.3 Area shaded by beam stop

Information lost in the stem of the beam stop area may be reconstructed from symmetry considerations. In the centre, information is lost without any possibility to recover it. When integrals are to be computed from the pattern, it will be useful to fill the blind hole in the middle by an extrapolated surface in order to minimise systematic errors.

5. Concept of masks

The evaluation steps discussed in Section 4 are coded as procedures for PV–WAVE. By my convention the names of these procedures begin with the characters "sf_". Some of the procedures need additional information, which must be supplied by the user. Information such as a mask is frequently requested. A mask is a special image, which only contains pixel values of *true* (1) or *false* (0).

Figure 2 shows the mask which can be generated by first copying the image (m = r480) to a mask image and then setting all intensities to *true*, which are greater than 300 counts (m.map=r480.map GT 300). In order to see the result as presented in figure 2 the

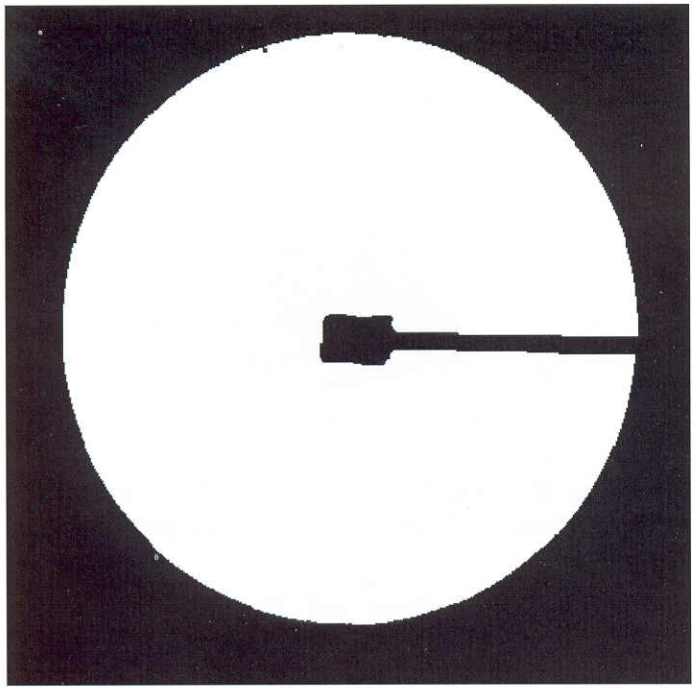

Figure 2: Example of a mask extracted from a SAXS pattern with fibre symmetry.

user types tvscl, m.map. This mask is good for the determination of the position of the scattering pattern on the image plate. Moreover, it can be used to set the noisy blind area to zero intensity (r480.map = r480.map * m.map).

Before the program can start to fill information into zero intensity pixels, the image must be centred and aligned. Masking m.map = r480.map GT 8000 yields the mask shown in figure 3. After manual erasure of the three fragments near the beam stop this mask can be used by an alignment procedure, which starts by computing centres of gravity from both the contiguous regions in the mask.

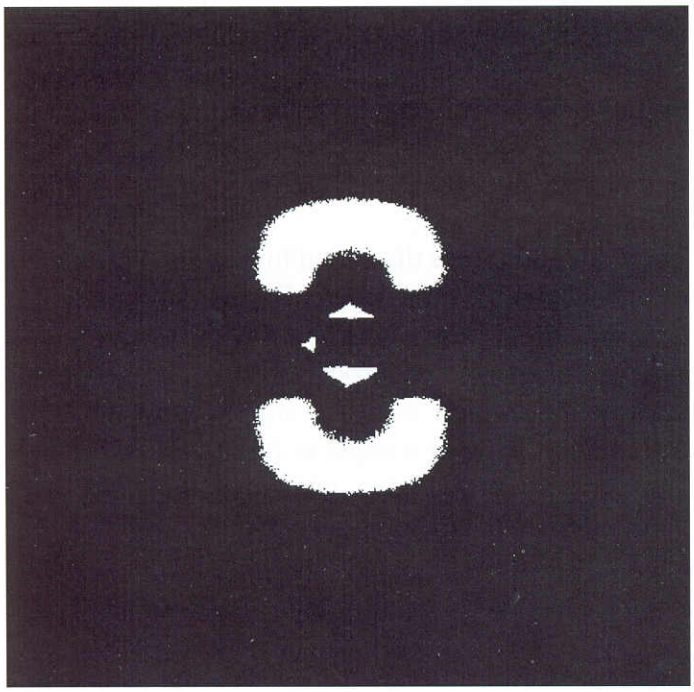

Figure 3: Mask for the alignment of SAXS patterns with fibre symmetry.

6. Filling in missing information

Now symmetry considerations can be used to fill some part of the blind area of the image, and the remaining part of the image may be filled with extrapolated surfaces using procedures provided in the IMSL library of PV-WAVE. A fair understanding of the advanced matrix operations built into PV-WAVE is essential for generating economical code for these algorithms. PV-WAVE code is interpreted, so there is considerable time penalty for inefficiency.

In particular, the 2D extrapolation of a surface into the outer blind area will be demonstrated. It is well known from quantitative analysis of 1D SAXS data that one should gather information on the shape of the SAXS curve over a wide angular range including

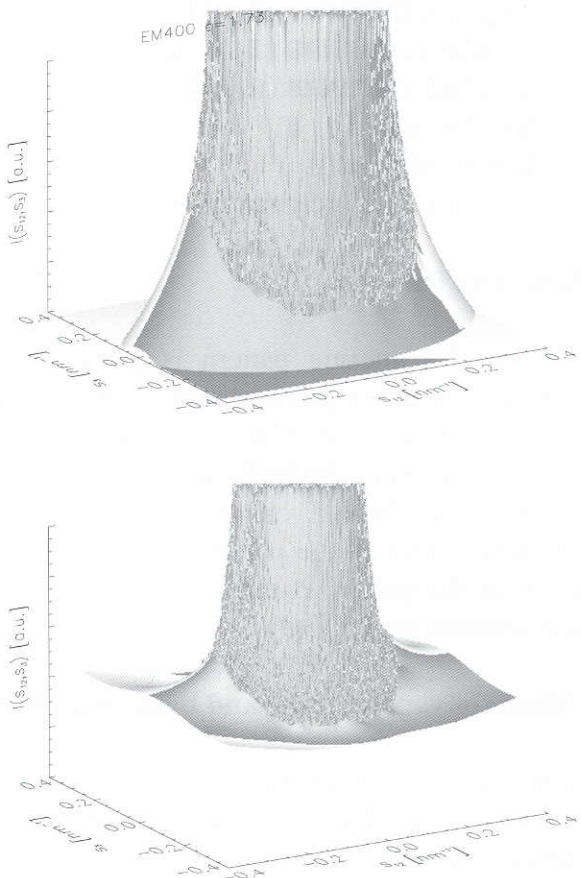

Figure 4: Examples of extrapolated aprons using 2D-SAXS data from different polyetheresters. Top: Arnitel A2000/20. Here the sample–detector distance is too long to give a reasonable 2D extrapolation. Bottom: PBT/PEG. In this series all the extrapolated aprons show the expected shape of a SAXS fluctuation background.

the beginning of the WAXS curve [1]. This ensures that the determination of the electron density fluctuation background is possible. If the measured data do not extend far enough into the region of Porod's law, one will have to guess the fluctuation background and information on the size distribution of domains is inaccessible.

An extrapolation may be superfluous, either if the vacuum tube can be widened without risking failure of the vacuum window, or if the distance between sample and detector can be shortened without loss of information in the central part, or if it is possible to measure the same state of the sample with two different instrument adjustments. The special benefit of a 2D extrapolation may result from the fact that the fitting of a surface to given points is stiffer than the 1D fitting of a curve. Thus it might follow the expected shape of a 2D SAXS pattern, if only the measured data are sufficient for a prediction. Since we generally record patterns from a series of states, we can compare the extrapolated aprons and thus obtain some heuristic measure on the validity of the extrapolations. Examples are shown in figure 4.

7. Evaluation of the patterns

In order to perform a qualitative evaluation of the patterns, one does not need to work through all the stages of preprocessing, which have been demonstrated here. Thus information on several general features of the domain structure and its response on straining can be obtained from simply picking the positions of peak maxima and plotting them versus the sample elongation [2].

Modelling of the 2D scattering pattern as a whole is a challenging task for future quantitative evaluation methods. But in analogy to the one-dimensional case, a quantitative evaluation can be performed on curves, which can be extracted from the scattering patterns by projection operations. Thus the "longitudinal structure" and the "transverse structure" of the fibre may be studied [3] by application of models which describe the hard domains and the soft domains in the elastomer by 1D or 2D models in real space. The scattering intensity of the longitudinal structure $I_1(s_3)$ is given by the projection

$$I_1(s_3) = \int_0^\infty s_{12} I(s_{12}, s_3) ds_{12}$$

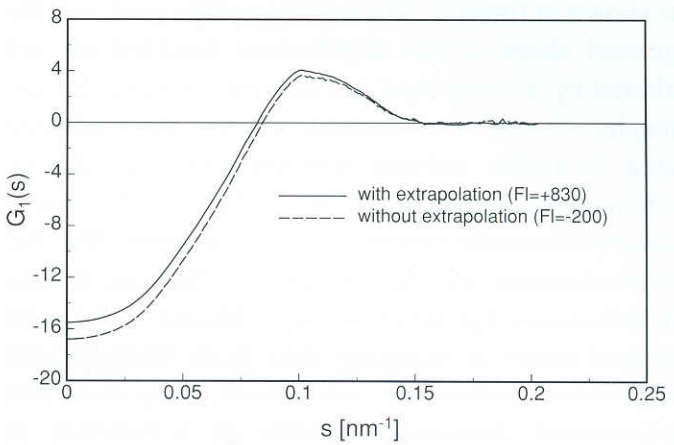

Figure 5: Interference function $G_1(s_3)$ computed from vertical projections $I_1(s_3)$ after correction for the scattering effects of non–ideal multiphase systems. Data from sample PBT/PEG at an elongation of ε=1.48.

of the pattern intensity $I(s_{12},s_3)$ and the scattering intensity of the transversal structure $I_2(s_{12})$ is defined by the projection integral

$$I_2(s_{12}) = \int_{-\infty}^{\infty} I(s_{12}, s_3) ds_3$$

The latter can be treated like any SAXS curve measured with the Kratky camera. Each of the two projections from the same scattering pattern has its own Porod law, and if the range of the measured data is insufficient for a complete evaluation of $I_1(s_3)$, the data in $I_2(s_{12})$ may still suffice for a quantitative evaluation of the transverse structure.

The effect of an insufficient measuring area can easily be demonstrated by comparing different evaluations of the same sample. One of the evaluations relies on the measured pattern, the second is based on the same data after extrapolation of an apron. In order to find Porod's law in the projection $I_1(s_3)$ obtained from the narrow area data, one has to assume a negative fluctuation background, which is of no physical sense. The corresponding projection from the wide area data shows a well expressed Porod law with a positive fluctuation background, if the shape of the apron made physical sense (as found for patterns from the sample PBT/PEG). Quantitative evaluation of the longitudinal structure is based on the analysis of an interference function $G_1(s_3)$ [4], in which the heights of the soft domains and the heights of the hard domains are given by attenuated cosine functions. The frequency of the cosine is related to the average domain height; the attenuation factor is related to the width of the domain height distribution. An example

is shown in figure 5. The position of the peak and the general shape of the interference function are not altered by missing data and thus the average domain heights should be extractable even if the measured area is rather narrow. On the other hand, the attenuation is considerably higher in the curve obtained from the narrow scattering pattern. Thus the determination of the width of domain height distributions becomes wrong. Model fitting on several series of straining data from thermoplastic elastomers confirm this assessment. They show that determined distribution widths as a function of elongation can only be connected by a smooth curve, if the previous analysis of the Porod region has been performed in a sufficiently long angular interval.

References

[1] Ruland, W., (1971) *J. Appl. Cryst.* **4**, 70-74

[2] Stribeck, N., Sapoundjieva, D., Denchev, Z., Apostolov, A.A., Zachmann, H.G., Stamm, M., Fakirov, S. (1997) *Macromolecules* **30**, 1329-1339

[3] Bonart, R. (1966) *Colloid Polym. Sci.*, **211**, 14-33

[4] Ruland, W. (1977) *Colloid Polym. Sci.* **255**, 417-427

Chain Mobility in Polymer Systems; Lamellar Doubling during Annealing of Polyethylene

S.Rastogi, A.B.Spoelstra, J.G.P.Goossens and P.J.Lemstra

Eindhoven Polymer Laboratories / The Dutch Polymer Institute (DPI), Eindhoven University of Technology, Department of Chemical Engineering, P.O. Box 513, 5600 MB Eindhoven, The Netherlands.

The motion of chains in quiescent polymer melts is confined to a reptative diffusion along the contour length as proposed by De Gennes [1,2]. In the constitutive equations based on the concept of chain reptation, it is assumed that the longest relaxation times in polymer melts correspond to the reptative motion of complete chains [3]. In the case of ultra-high molecular weight polyethylene, UHMW-PE, the experimentally determined [4,5] longest relaxation times exceed 10^4 seconds.

Processing of UHMW-PE via conventional routes is virtually impossible due to the high molar mass and the excessive high melt-viscosity. The viscosity of polymer melts, above a certain threshold value for the molar mass M_c, is given by $\log \eta_0 = C + 3.4 \log M_w$, where η_0 is the zero-shear viscosity. The strong increase in the melt-viscosity with increasing molar mass is related to entanglement coupling [6] and the presence of a physical entanglement network.

Despite many efforts in the past, no advantage could be gained by processing disentangled solution-crystallised UHMW-PE via the melt. We anticipated an initial lower melt-viscosity upon heating disentangled UHMW-PE above the melting temperature in view of the fact that a certain time period is needed to form an equilibrium melt starting from (completely) disentangled systems.

Since the long chains in UHMW-PE have to reptate into each other and the tube renewal time is expected to be relatively long, in the order of a few hours [6], welding or sintering of the UHMW-PE is practically not feasible via conventional routes. In this letter, we present a summary of our recent study on enhanced chain mobility during annealing in a temperature range close to, but below the melting point of solution-crystallised UHMW-PE. The achieved chain mobility is used in welding of the two UHMW-PE films.

Characterisation techniques

By proper crystallisation from semi-dilute solutions of UHMW-PE ($M_w \sim 3 \times 10^3$ kg mol, Hoechst GUR 2122), we could make films possessing well stacked lamellar crystals. By combining small-angle X-ray scattering (SAXS), Transmission Electron Microscopy (TEM) and Low-frequency Raman spectroscopy the confined motion of the polymer chains along the chain axis has been traced.

The SAXS/WAXS studies were performed at station 8.2 of the synchrotron radiation facility available in Daresbury, U.K. [7]. A Linkam THMS 600 hot-stage mounted on the optical bench with a sample holder (capillary/film) was used to perform heating, cooling or annealing experiments. The SAXS and WAXS detectors were calibrated using the usual standards. Experimental data were normalised for the transmitted intensity and corrected for detector response and the background scattering.